Size-dependent lattice structure of palladium studied by x-ray absorption spectroscopy

Chih-Ming Lin,[1,*] Tsu-Lien Hung,[2] Yen-Heng Huang,[3] Kung-Te Wu,[4] Mau-Tsu Tang,[5] Chih-Hao Lee,[3] C. T. Chen,[6] and Y. Y. Chen[6]

[1]*Department of Applied Science, National Hsinchu University of Education, Hsinchu 30014, Taiwan, Republic of China*
[2]*Department of Physics, National Tsing-Hua University, Hsinchu 30013, Taiwan, Republic of China*
[3]*Department of Engineering and System Science, National Tsing-Hua University, Hsinchu 30013, Taiwan, Republic of China*
[4]*Department of Physics, Soochow University, Taipei, Taiwan, Republic of China*
[5]*National Synchrotron Radiation Research Center, Hsinchu 30076, Taiwan, Republic of China*
[6]*Institute of Physics, Academia Sinica, Taipei, Taiwan, 11529, Republic of China*

X-ray absorption spectroscopy measurements have been made on 7-, 12-, and 23-nm palladium particles, along with bulk material as reference. With decreasing particle size, the extended x-ray absorption fine spectra reveal a substantial contraction of the nearest-neighbor distance and a reduction of the average coordination number, but an increasing Debye-Waller factor. Meanwhile, the x-ray absorption near edge spectra show a decreasing density of unoccupied states with decreasing particle size.

Intensive research efforts have been focused on the physical and chemical properties of metal nanoparticles, which are also referred to often as small metal clusters.[1–9] Controlling the particle size d is a key theme, since it affects significantly the optical, magnetic, electronic, or catalytic behavior of nanostructured materials. On a more fundamental level, the size dependence of nearest-neighbor distance R is one of the most important issues in applications to mesoscopic devices. This paper reports our effort in elucidating the size dependence of R and related properties in substrate-free palladium nanoparticles by x-ray absorption spectroscopy (XAS) measurements.

In past decades, nanoparticles have been studied by several different experimental techniques. The electronic structure of Pd nanoparticles, which were supported on amorphous carbon substrates, was first investigated by Mason *et al.*[1] using x-ray photoemission spectroscopy. XAS experiments were carried out to observe the contraction of nearest-neighbor distance R of small metal clusters prepared under vacuum evaporation,[2,9] in catalytic systems,[3,5,6] or in rare-gas matrices.[4,7] According to Apai *et al.*,[2] for small Cu and Ni clusters, the increased *K*-edge threshold energy and the contracted R are caused by the size-dependent renormalization of valence electron charge.[2] This was further explained by the increased surface-to-volume ratio with decreasing cluster size, resulting in a more free-atom-like configuration of the metal atoms.[2] Recently, Balerna *et al.*[9] connected the contraction of nearest-neighbor distance to the surface stress caused by the large surface-to-volume ratio in terms of a liquid drop model.[10] Panfilis *et al.*[11] also showed that a reduction in the average coordination number N was expected on general grounds for an aggregate of nanoclusters due to the reduced N value of surface atoms and the high average surface-to-volume ratio in nanophase palladium. The fact that all aforementioned studies involve substrates or matrices, which unavoidably cause a certain level of micrograins, disorder, defects, oxidation, and intergrain boundaries in any metal nanoparticles, leads to this study on substrate-free Pd. Along this line, a substrate-free approach has been used on small metal clusters in mesoscopic studies.[12,13]

The second critical issue being addressed in this work deals with the detailed lattice structure in nanoparticles. The conventional x-ray diffraction (XRD) and electron diffraction techniques measure the shift of x-ray or electron Bragg-diffraction peaks relative to those of the same material in bulk form.[2] It is well-known that such diffraction patterns provide only the long-range-ordered structure, which is sufficient for single crystal or bulk materials. However, for nanoparticles, they lack the ability to identify the local environment-sensitive short-range order. Other standard techniques such as the transmission electron microscopy (TEM)[14] provide only qualitative information through intensity contrast in nanoparticles. Consequently, in this work, XAS measurements were carried out to evaluate the size-dependent R value and *K*-edge threshold energy in substrate-free Pd nanoparticles.

Three Pd nanoparticle samples of different sizes were fabricated on a liquid-nitrogen-cooled cold trap by thermal evaporation in a $1-100$-torr helium atmosphere.[12,13] Figure 1 shows the XRD patterns of Pd bulk and the nanoparticle samples at ambient condition. Eight reflection indexes of (111), (200), (220), (311), (222), (400), (331), and (420) were identified by the cubic phase of Pd (card 05-0681 in the
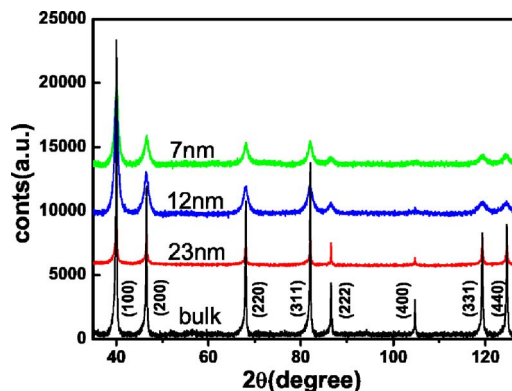

FIG. 1. (Color online) XRD spectra of bulk and 7-, 12- and 23-nm Pd particles at 300 K.
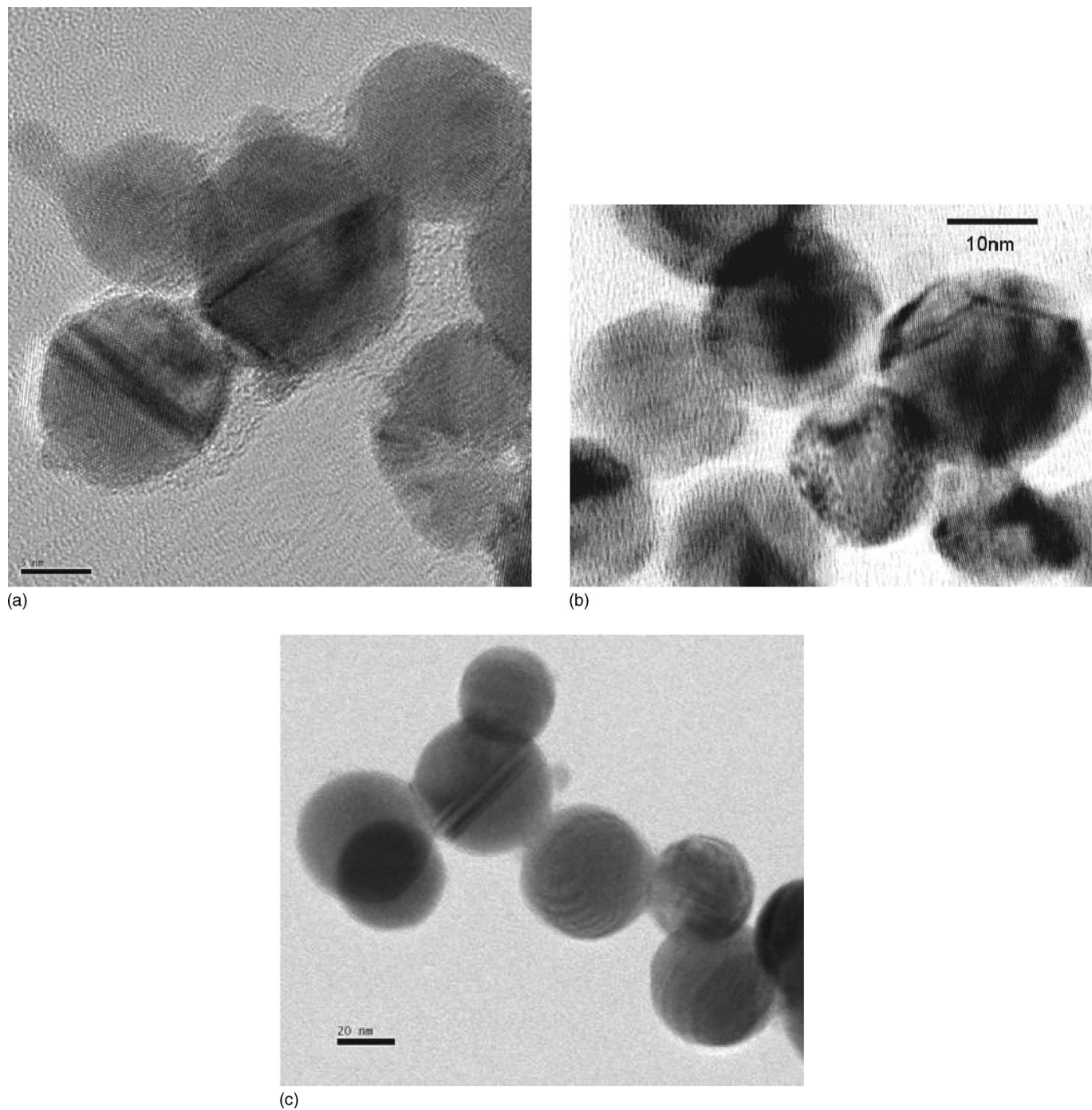
FIG. 2. TEM images of (a) 7-nm, (b) 12-nm, and (c) 23-nm Pd particles.

JCPDS file). The average size d of 7, 12, or 23 nm for each sample was calculated from the peak width of diffraction peaks. They are in good agreement with that obtained directly from TEM images in Fig. 2. The lattice parameters of 3.888, 3.889, 3.889, and 3.888 Å thus obtained for the 7-, 12-, and 23-nm particles and the bulk, respectively, remain practically the same.

The Pd *K*-edge (E_K=24.350 keV) x-ray absorption spectra were collected from the beamline BL12B2 at the SPring-8, Hyogo, Japan. The electron storage ring was operated at 8 GeV. A double Si(111) crystal monochromator was employed for energy selection. With all XAS measurements performed in a transmission mode, three gas-filled ionization chambers were used in series to measure the absorption intensities of the sample and Pd foil as a reference standard. Each sample was placed between the incident beam detector and the reference beam detector. The sample preparation, control of parameters for extended x-ray absorption fine spectra (EXAFS) measurements, and data collection modes were all done as per the guidelines set by the International XAFS Society Standards and Criteria Committee.[15,16] For analyzing the XAS data, the raw absorption spectrum in the
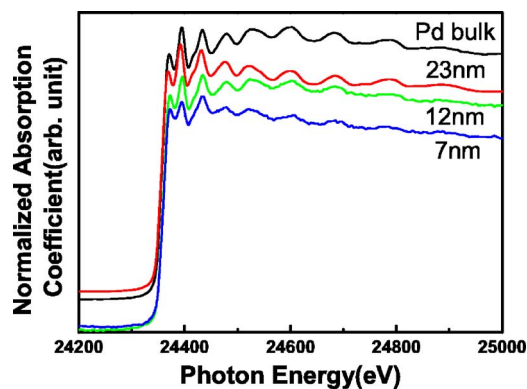
FIG. 3. (Color online) Normalized K-edge absorption coefficients of Pd samples at 300 K. The energy at the edge inflection point is 24 350 eV.

preedge region was fitted to a straight line and the background above the edge was fitted using a 7-knot cubic spline function calculated from the AUTOBK program in FEFF-8.[17] The EXAFS function, χ, was obtained by subtracting the postedge background from the overall absorption and then normalized with respect to the edge jump step. The normalized $\chi(E)$ was transformed from energy space to k-space, where k is the photoelectron wave vector. The $\chi(k)$ data were multiplied by k^1 to compensate for the damping of EXAFS oscillations in the high k-region. Subsequently, k^1-weighted $\chi(k)$ data in the k-space ranging from 3.05 to 10.75 Å^{-1} for the Pd K-edge were Fourier transformed (FT) to r-space to separate the EXAFS contributions from the different coordination shells. A nonlinear least-squares algorithm was applied to the curve fitting of an EXAFS in the r-space between 2.2 and 3.0 Å (without phase correction) for Pd. All computer programs were implemented in the UWXAFS 3.0 package[18] with the backscattering amplitude and the phase shift for the specific atom pairs being theoretically calculated by using FEFF-8 code.[17] From these analyses, structural parameters including N, R, and the Debye-Waller factor σ^2 were calculated. The amplitude reduction factor, S_0^2, was obtained by analyzing the Pd foil and by fixing coordination numbers in the FEFFIT input file. The S_0^2 value was found to be 0.8 for all samples.

X-ray absorption spectra are shown in Figs. 3 and 4. Figure 3 shows normalized K-edge absorption coefficients of Pd samples at 300 K. Figure 4(a) shows the weighted EXAFS spectra $k^1\chi(k)$ versus k, and Fig. 4(b) gives the Fourier-transformed and k^1-weighted EXAFS spectra (Δk =3.05–10.75 Å^{-1}). A peak between 2.2 and 3.0 Å in Fig. 4(b) corresponds to the nearest-neighbor distance R. It is evident that, as d decreases, there is an increased K-edge threshold energy and a shift of the Fourier-transformed main peak towards smaller R. Their values are summarized in Table I. Figure 5(a) shows the contraction of nearest-neighbor distance ΔR ($R_{bulk}-R_{nanoparticle}$) as a linear function of the inverse of average particle size 1/d, conforming with the earlier observations of Apai et al.[2] and Balerna et al.[9] Such a lattice contraction in Pd is also similar to that of closely packed nanoparticles studied by Mays et al.[10] using electron microscopy. Their results[2,9,10] indicate that, from a
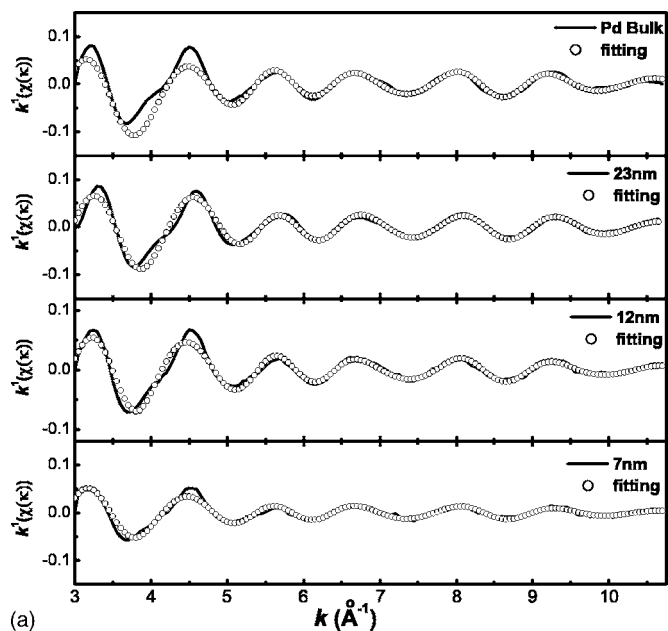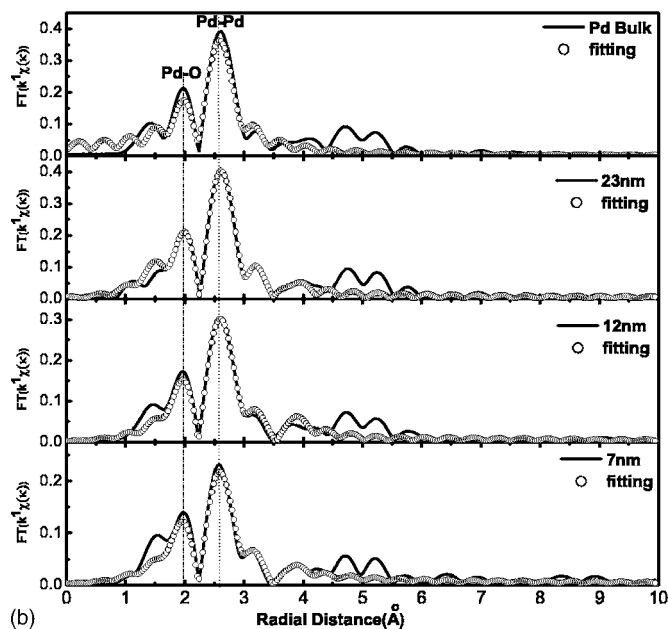
FIG. 4. (a) Weighted EXAFS spectra as k-dependence of $k^1\chi(k)$. (b) Fourier-transformed k^1-weighted EXAFS spectra (Δk =3.23–10.86 Å^{-1}).

macroscopic point of view, ΔR is related to surface stress caused by a high surface-to-volume ratio in the clusters. Accordingly, following a liquid drop model,[2,9]

$$\Delta R = -(4/3)KfR_b/d, \qquad (1)$$

where d is the average particle size, f the surface stress, R_b the nearest-neighbor distance in bulk material, and K the bulk compressibility. The slope of the straight line fit in Fig. 5(a) is 0.0065 for Pd, which is about 2.5 times 0.0023 for Au nanoparticles.[9] The bulk values of R_b (Refs. 19 and 20) and K (Ref. 21) for Pd (2.75 Å and 1/180 GPa) and Au (2.885 Å and 1/220 GPa) yield an approximately 15% higher R_bK

TABLE I. Particle size, nearest-neighbor distance, Debye-Waller factor, and coordination number of bulk and nanoparticle palladium.

d	$R(k)$ (Å) (± 0.01)	σ^2 (Å^2) ($\pm 20\%$)	N
7 nm	2.724	0.01001	11.6
12 nm	2.736	0.00783	11.8
23 nm	2.742	0.00559	11.96
bulk	2.757	0.00548	12.0

product in Eq. (1) for Pd than that for Au. It implies that the surface stress f in substrate-free Pd is larger than that of Au nanoparticles prepared by evaporation under vacuum. This can be explained by the increased surface-to-volume ratio and free-atom-like configuration of the substrate-free nanoparticles with increasing particle size reduction.[2]

Experimentally derived mean coordination numbers for substrate-free Pd nanoparticles in Fig. 5(b) and Table I appear to agree with that in earlier reports[8,9] for metal nanoparticles on weakly interacting substrates. However, up to now, controversies remain for the R variation in metal nanoparticles prepared by evaporation under vacuum.[3,5,6,22] While some indicated similar R values for nanoparticles and the bulk,[3,5,6,22] others showed R reduction.[4,7,9] The different behaviors could be due to different metal-substrate interactions.[9] More relevant to this work is the uncertainty still existing in the case of Pd.[23–25] For ligand-stabilized Pd nanoparticles, R values are comparable to R_b.[23] For polymer-protected species,[24] R increases with particle size reduction. Heinemann *et al.*,[26] Lamber *et al.*,[27] Kuhrt *et al.*,[28] and Goyhenex *et al.*[29] also reported larger R values than R_b in Pd nanoparticles on various substrates.

The particle size dependence of the Debye-Waller factor σ^2 is given in Fig. 5(c). It increases from 0.005 48 Å^2 for the bulk to 0.005 59 Å^2 at d=23 nm, followed by a rapid increase to 0.010 Å^2 as d further decreases to 7 nm. The result is similar to that of Moraweck *et al.*,[30] who reported that Debye-Waller factors in small Pd particles in the framework of a Y-zeolite were larger than that of the bulk material.

In all earlier studies,[8,9,30] metal nanoparticles were on some sorts of substrates, which are expected to have influence on R, N, and σ^2. Our data of decreasing R and N, along with increasing σ^2 with decreasing d are direct observations in substrate-free Pd nanoparticles. Actually, in addition to experimental evaluations, theoretical studies were also performed by using a linear combination of Gaussian-type orbitals, fitting-functions, and density-functional (LCGTO-FF-DF) approach.[31,32] Based on Pd particles of 4 to 309 atoms each, Krüger *et al.*[32] show clearly a contraction of the average R value with decreasing particle size. In agreement with this theoretical work, our experimental observation of the R reduction with decreasing d in substrate-free Pd is likely an intrinsic property of Pd nanoparticles.

Figure 6 shows Pd *K*-edge x-ray absorption near edge spectra (XANES) of 7-, 12-, and 23-nm nanoparticles at 300 K, with the bulk as reference. The energy was calibrated
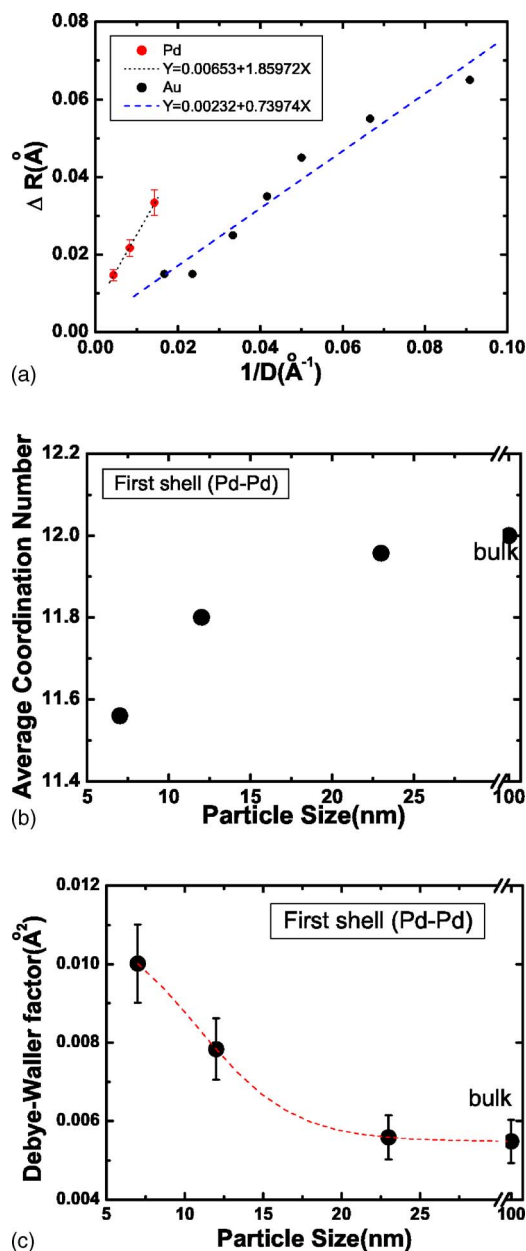

FIG. 5. (Color online) (a) Nearest-neighbor distance contraction versus the inverse of Pd particle size. (b) Average coordination number versus Pd particle size. (c) Debye-Waller factor versus Pd particle size.

using the data acquired simultaneously on a Pd foil at 300 K. The absorption transition in the preedge region is a 1s to 4d dipole forbidden transition according to the selection rule, $\Delta l = 1$ and $\Delta j = 1$, where l and j are the orbital angular momentum and the total angular momentum of the local density of states, respectively. The positions of the $1s \rightarrow 5p$, pd, and $1s \rightarrow 4f$, pf[33–35] resonance peaks in the XANES are shifted downward relative to that of Pd bulk. The data indicate that they result from lattice contraction.[35] This is consistent with the result of the R reduction mentioned above. The electronic structure of Pd nanoparticles is of interest for understanding the substrate-free nanoparticles. On the other hand, x-ray-absorption spectroscopy at the *K* and *L* edges has been used
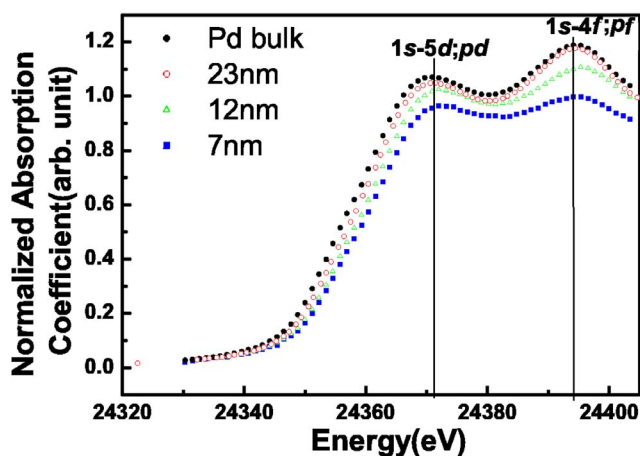
FIG. 6. (Color online) K-edge XANES spectra of Pd samples at 300 K.

to probe the density of states above the Fermi level.[36] Paolucci *et al.*[37] indicated that, for light elements, the K-edge spectra can provide a precise measurement of the density of unoccupied p states because the K-hole lifetime broadening is small. For heavier elements such as the 4d series, this lifetime broadening is large (~ 6 eV),[26] so that K-edge measurements are restricted to 3d and lighter elements. Because of the lifetime broadening and limited spectrometer resolution, Pd K-edge XANES spectra provide only little informa-tion. However, from our previous study on Pd nanoparticles,[12,13] the Sommerfeld constant of electronic specific heat decreases to a lower value than that of the bulk, implying an overall decrease of the electronic density of states at the Fermi level in Pd nanoparticles. The density of states of unoccupied states decreases with size reduction can be then concluded.

In summary, we have demonstrated the substrate-free effect in 7-, 12- and 23-nm palladium particles by K-edge x-ray absorption spectroscopy measurements. From EXAFS spectra, the nearest-neighbor distance and the mean coordination number decrease, while the Debye-Waller factor increases with decreasing nanoparticle size. In contrast to some earlier reports of increasing nearest-neighbor distance in metal nanoparticles on substrates, the difference is believed to reflect interactions with the substrate. In addition, from XANES spectra, with decreasing particle size, a reduction in the density of states of unoccupied states is observed.

*Corresponding author.
[1] M. G. Mason, L. J. Gerenser, and S. T. Lee, Phys. Rev. Lett. **39**, 288 (1977).
[2] G. Apai, J. F. Hamilton, J. Stohr, and A. Thompson, Phys. Rev. Lett. **43**, 165 (1979).
[3] G. H. Via, J. H. Sinflet, and F. W. Lytle, J. Chem. Phys. **71**, 690 (1979).
[4] P. A. Montano and G. K. Shenoy, Solid State Commun. **35**, 53 (1980).
[5] J. H. Sinflet, G. H. Via, F. W. Lytle, and R. B. Greegor, J. Chem. Phys. **75**, 5527 (1981).
[6] J. H. Sinflet, G. H. Via, and F. W. Lytle, J. Chem. Phys. **76**, 2779 (1982).
[7] H. Purdum, P. A. Montano, G. K. Shenoy, and T. Morrison, Phys. Rev. B **25**, 4412 (1982).
[8] M. G. Mason, Phys. Rev. B **27**, 748 (1983).
[9] A. Balerna, E. Bernieri, P. Picozzi, A. Reale, S. Santucci, E. Burattini, and S. Mobilio, Phys. Rev. B **31**, 5058 (1985).
[10] C. W. Mays, J. S. Vermaak, and D. Kuhlmann-Wilsorf, Surf. Sci. **12**, 134 (1968).
[11] S. D. Panfilis, F. D'Acapito, V. Haas, H. Konrad, J. Weissmüller, and Boscherini, Mater. Sci. Forum **195**, 67 (1995).
[12] Y. Y. Chen, Y. D. Yao, S. S. Hsiao, S. U. Jen, B. T. Lin, H. M. Lin, and C. Y. Tung, Phys. Rev. B **52**, 9364 (1995).
[13] Y. Y. Chen, Y. D. Yao, S. U. Jen, B. T. Lin, H. M. Lin, C. Y. Tung, and S. S. Hsiao, Nanostruct. Mater. **6**, 605 (1995).
[14] Y. Sun, A. I. Frenkel, R. Isseroff, C. Shonbrun, M. Forman, K. Shin, T. Koga, H. White, L. Zhang, Y. Zhu, M. H. Rafailovich, and J. C. Sokolov, Langmuir **22**, 807 (2006).
[15] http://ixs.iit.edu/subcommittee_reports/sc/sc00report.pdf
[16] http://ixs.iit.edu/subcommittee_ reports/sc/err-rep.pdf
[17] S. I. Zabinsky, J. J. Rehr, A. L. Ankudinov, R. C. Albers, and M. J. Eller, Phys. Rev. B **52**, 2995 (1995).
[18] E. A. Stern, M. Newville, B. Ravel, Y. Yacoby, and D. Haskel, Physica B **208-209**, 117 (1995).
[19] Sven Krüger, Stefan Vent, Folke Nörtemann, Markus Staufer, and Notker Rösch, J. Chem. Phys. **115**, 2082 (2001).
[20] N. Nilius, T. M. Wallis, and W. Ho, Science **297**, 1853 (2002).
[21] G. Simmons and H. Wang, *Single Crystal Elastic Constants and Calculated Aggregate Properties: A Handbook*, 2nd ed. (MIT Press, Cambridge, MA, 1971); D. L. Heinz and R. Jeanloz, J. Appl. Phys. **55**, 885 (1984).
[22] P. Lagarde, T. Murata, G. Vlaic, E. Freund, H. Dexpert, and J. P. Bounouville, J. Catal. **84**, 333 (1983).
[23] R. E. Benfield, A. Filipponi, D. T. Bowron, R. J. Newport, S. J. Gurman, and G. Schmid, Physica B **208/209**, 671 (1995).
[24] T. Teranishi and M. Miyake, Chem. Mater. **10**, 594 (1998).
[25] R. Lamber, S. Wetjen, and N. I. Jaeger, Phys. Rev. B **51**, 10968 (1995).
[26] K. Heinemann and H. Poppa, Surf. Sci. **156**, 265 (1985).
[27] R. Lamber, N. Jaeger, and G. Schulz-Ekloff, Surf. Sci. **227**, 15 (1990).
[28] C. Kuhrt and R. Anton, Thin Solid Films **198**, 301 (1991).
[29] C. Goyhenex, C. R. Henry, and J. Urban, Philos. Mag. A **69**,

1073 (1994).

[30] B. Moraweck and A. J. Renouprez, Surf. Sci. **106**, 35 (1981).

[31] B. I. Dunlap and N. Rösch, Adv. Quantum Chem. **21**, 317 (1990).

[32] S. Krüger, S. Vent, F. Nörtemann, M. Staufer, and N. Rösch, J. Chem. Phys. **115**, 2082 (2001).

[33] J. E. Müller, O. Jepsen, O. K. Andersen, and J. W. Wilkins, Phys.

Rev. Lett. **40**, 720 (1978).

[34] J. A. McCaulley, Phys. Rev. B **47**, 4873 (1993).

[35] J. A. McCaulley, Phys. Rev. B **48**, 666 (1993).

[36] T. K. Sham, Phys. Rev. B **31**, 1888 (1985).

[37] G. Paolucci, K. C. Prince, G. Comelli, A. Santoni, and O. Bisi, Phys. Rev. B **41**, 3862 (1990).